Association of high gene expression levels of *ARF6* with the immune microenvironment and prediction of poor outcomes

Natsuko Kawanishi,[1] Yasmine Baca,[2] Joanne Xiu,[2] Hiroyuki Arai,[1] Francesca Battaglin,[1] Priya Jayachandran,[1] Shivani Soni,[1] Wu Zhang,[1] Philip A. Philip,[3] Davendra Sohal,[4] Moh'D Khushman,[5] Benjamin A. Weinberg,[6] Michael J. Hall,[7] David Park,[8] Emil Lou,[9] Anthony F. Shields,[3] A. Craig Lockhart,[10] W. Michael Korn,[2] Heinz-Josef Lenz[1]

1. Division of Medical Oncology, Norris Comprehensive Cancer Center, Keck School of Medicine, University of Southern California, Los Angeles, CA; 2. Caris Life Sciences, Phoenix, AZ; 3. Department of Oncology, Karmanos Cancer Institute, Wayne State University, Detroit, MI; 4. Department of Hematology/Oncology, University of Cincinnati, Cincinnati, OH; 5. Department of Medical Oncology, Mitchell Cancer Institute, University of South Alabama, Mobile, AL; 6. Ruesch Center for the Cure of Gastrointestinal Cancers, Lombardi Comprehensive Cancer Center, Georgetown University Medical Center, Washington, DC; 7. Department of Medical Oncology, Fox Chase Cancer Center, Philadelphia, PA; 8. St Jude Crosson Cancer Institute/St Joseph Heritage Healthcare, Fullerton, CA; 9. University of Minnesota, Minneapolis, MN; 10. Division of Oncology, University of Miami Miller School of Medicine, Miami, FL.

Keck School of Medicine of USC

CARIS POA™ PRECISION ONCOLOGY ALLIANCE

 # 3092

Introduction

ADP-ribosylation factor 6 (*ARF6*) is a member of small GTPase *ARF*s in the *RAS* superfamily. They conduct the fundamental biological processes, such as cytokinesis, cell adhesion, and cell growth, which are regulated by various mediators.

Only ARF6 is localized and functions at cell membranes regulating membrane trafficking, remodeling, and tumor progression [1].

Preclinical study shows that *TP53* and *KRAS* in pancreatic ductal adenocarcinoma (PDAC) cooperatively activate the *ARF6-AMAP1* pathway which serves as a link by which pancreatic driver mutations promote tumor malignant potential such as fibrosis and invasion, encouraging PD-L1 dynamics and immune evasion properties.

High expression in IHC of *ARF6* pathway components in KPC cells indicate poor prognoses [2].

The clinical impact of *ARF6* expression on progression and prognosis in PDAC is still largely unknown.

Methods

- A total of 2,948 PDAC samples were analyzed using next-generation sequencing of RNA (whole transcriptome, NovaSeq) and DNA (NextSeq, 592 genes or NovaSeq, whole exome sequencing), and immunohistochemistry (IHC) (Caris Life Sciences, Phoenix, AZ).
- *ARF6* gene expression transcripts per million (TPM) were stratified into quartiles for analysis (Q1–Q4).
- QuantiSeq (Finotello 2019, Genome Medicine) was used for the quantification of the tumor infiltrating immune contexture using transcriptomic data.
- Overall survival (OS) was obtained from insurance claims data and Kaplan-Meier estimators were calculated for molecularly defined patient cohorts.
- *P*-values were adjusted for multiple comparisons, and q<0.05 was considered significant.

Results

Table 1. Patient characteristics

ARF6 quartiles	N / Average age				
	Female (%)		Male (%)		Total
Q1	332 (45.0)	66.4	405 (55.0)	63.6	737
Q2	343 (46.5)	65.5	394 (53.5)	65.4	737
Q3	346 (46.9)	66.5	391 (53.1)	65.2	737
Q4	337 (45.7)	66.2	400 (54.3)	65.8	737
Total	1358		1590		2948

Patients were divided equally into four groups according to their expression levels.
QL: lowest expression quartile; QH: highest expression quartile (Q1–Q4)
There were no significant differences among patient clinical characteristics.

Results

Table 2. Metastatic distributions TPM compared to primary/local tumors

	N	Median TPM	*P*-value		N	Median TPM	*P*-value
Primary / local	1268	27.6	—	**Metastatic**	1680	33.7	***q*<0.05**
Liver	1038	36.2	***q*<0.05**	Gastroesophageal	18	29.5	**0.62**
Peritoneal	166	27.1	**0.72**	Large intestine	16	32.3	**0.35**
Small intestine	106	29.8	**0.37**	Lung	14	29.8	**0.16**
Abdomen	89	25.8	**0.65**	Lymph node	12	34.3	**<0.05**
Adrenal grand	64	36.3	**0.37**	Ovary/Uterus	9	31.9	**0.82**
Biliary tree	53	25.8	**0.94**	Pelvis	8	28.3	**0.68**
Bone	36	36.4	**<0.05**	Skin	6	64.3	**<0.05**
Connective tissue	33	33.1	**0.14**	Other	12	34.1	**0.08**

ARF6 expression in TPM was higher in metastases compared to that in primary/local tumors (***q*<0.05**).
Specific metastatic sites showed higher expression TPM in **liver** (***q*<0.05**), **skin**, **bone**, and **lymph nodes** than in primary/local tumors (all ***p*<0.05**).

Figure 1. Significant and trending genetic alterations

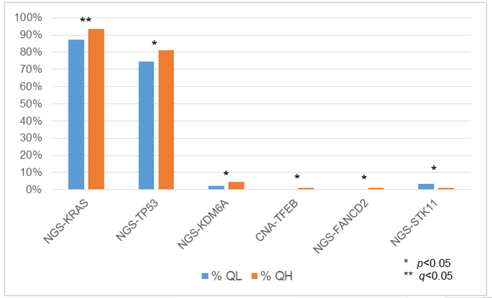

	%QL	%QH			%QL	%QH	
NGS-KRAS	87.2	93.4	***q*<0.05**	**NGS-FANCD2**	0.0	0.9	***p*<0.05**
NGS-TP53	74.7	81.1	***p*<0.05**	**CNA-TFEB**	0.0	1.2	***p*<0.05**
NGS-KDM6A	2.2	4.4	***p*<0.05**	**NGS-STK11**	3.3	1.2	***p*<0.05**

Mutations in ***KRAS*** were significantly more prevalent in QH than in QL (***q*<0.05**), and those in ***TP53*** trended similarly (***p*=0.0078**).

Compared to QL, *ARF6* QH tumors showed higher rates of mutations of ***KDM6A*** and ***FANCD2***, and ***TFEB*** amplifications. The ***STK11*** mutation rate tended to be lower in QH than in QL.

Figure 2. Expression levels of immune oncological markers and immune checkpoint genes

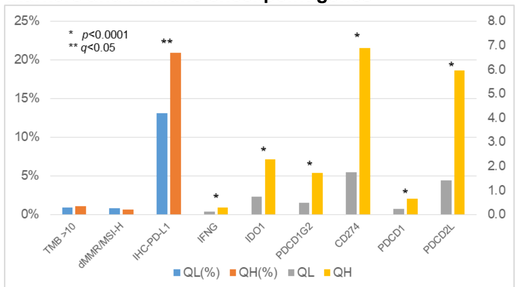

	% QL	% QH			QL	QH	
TMB≧10	0.9%	1.1%	0.715	***IFNG***	0.12	0.28	***q*<0.05**
dMMR/MSI-H	0.8%	0.6%	0.745	***IDO1***	0.73	2.27	***q*<0.05**
IHC-PD-L1	13.1%	20.9%	***q*<0.05**	***PDCD1G2***	0.48	1.72	***q*<0.05**
				CD274	1.76	6.89	***q*<0.05**
				PDCD1	0.22	0.66	***q*<0.05**
				PDCD2L	1.42	5.96	***q*<0.05**

PD-L1 expression by IHC was significantly higher in QH than in QL (***q*<0.05**).
Immune checkpoint genes by RNA expression (listed above)
All showed significantly higher expression levels in QH than in QL (***q*<0.05**).

Figure 3. Immune cell infiltrates and populations

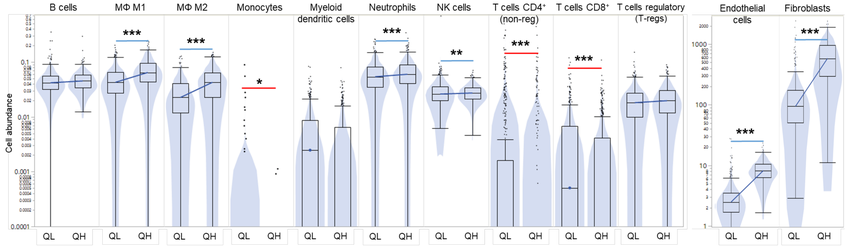

The tumor microenvironment (TME) characterization showed that **macrophages**, **neutrophils**, **NK cells**, **endothelial cells**, and **fibroblasts** were more abundant in QH than those in QL (all ***q*<0.05**).

CD4⁺ and **CD8⁺ T cells** were lower in QH (***q*<0.05**), and **monocytes** had similar trends (***p*<0.05**).

Figure 4. Overall survival compared tumors with *ARF6* expression levels

(A) OS among all tumors

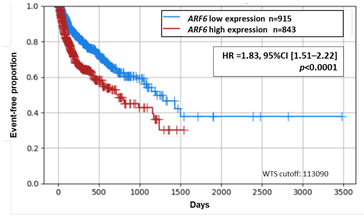

High-expressed *ARF6* tumors were **significantly associated with unfavorable OS** compared to low expressed tumors (**A**, ***p*<0.0001**).

The same effect was seen in OS when looking at **(B)** primary and **(C)** metastatic tumors separately.

Metastatic tumors with high *ARF6* expression showed a stronger unfavorable prognosis than did primary tumors considering their *p*-values (***p*=0.02 for primary** and ***p*<0.0001 for metastatic**, respectively).

(B) OS in primary tumors

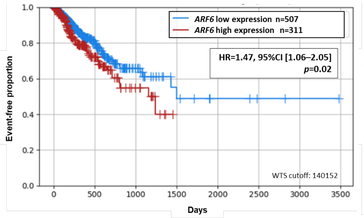

(C) OS in metastatic tumors

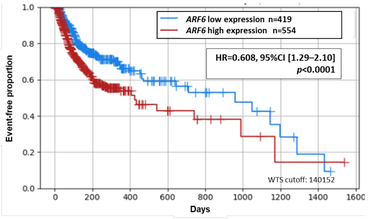

Conclusions

ARF6 expression in PDAC was significantly higher in metastatic tumors compared to primary and local tumors. High-expressed *ARF6* tumors demonstrated unfavorable OS as well as different tumor mutational and immune profiles.

These results provide the first clinical evidence supporting the *ARF6* pathway as a major downstream target of *KRAS* and *TP53* mutations promoting immune evasion, proving that *ARF6* is a novel marker for prognosis and a potential target for immune therapeutic strategies in PDAC.

References

1. Grossmann AH, et al. Small GTPases. 2019;10:1–12.
2. Hashimoto S, et al. Proc Natl Acad Sci USA. 2019;116:17450–9.

Email: knatsuko@kitasato-u.ac.jp